ELSEVIER

SCIENCE DIRECT®

PHYSICS LETTERS B

Physics Letters B 618 (2005) 209–220

www.elsevier.com/locate/physletb

NLO supersymmetric QCD corrections to $t\bar{t}h^0$ associated production at hadron colliders

Peng Wu [b], Wen-Gan Ma [a,b], Hong-Sheng Hou [b], Ren-You Zhang [b], Liang Han [b], Yi Jiang [b]

[a] *CCAST (World Laboratory), P.O. Box 8730, Beijing 100080, People's Republic of China*

[b] *Department of Modern Physics, University of Science and Technology of China (USTC), Hefei, Anhui 230027, People's Republic of China*

Received 2 February 2005; accepted 6 May 2005

Available online 23 May 2005

Editor: T. Yanagida

Abstract

We calculate NLO QCD corrections to the lightest neutral Higgs boson production associated with top quark pair at hadron colliders in the minimal supersymmetric standard model (MSSM). Our calculation shows that the total QCD correction significantly reduces its dependence on the renormalization/factorization scale. The relative correction from the SUSY QCD part approaches to be a constant, if either M_S or $m_{\tilde{g}}$ is heavy enough. The corrections are generally moderate (in the range of few percent to 20%) and under control in most of the SUSY parameter space. The relative correction is obviously related to $m_{\tilde{g}}$, A_t and μ, but not very sensitive to $\tan\beta$, M_S at both the Tevatron and the LHC with our specified parameters.

PACS: 12.60.Jv; 14.80.Cp; 14.65.Ha

1. Introduction

One of the major objectives of future high-energy experiments is to search for scalar Higgs particles and investigate the symmetry breaking mechanism of the electroweak interactions. In the standard model (SM) [1], one doublet of complex scalar fields is introduced to spontaneously break the symmetry, leading to a single neutral Higgs boson h^0. But there exists the problem of the quadratically divergent contributions to the corrections to the Higgs boson mass. This is the so-called naturalness problem. One of the hopeful methods, which can solve this problem, is the supersymmetric (SUSY) extension to the SM. In these extension models, the quadratic divergences

E-mail address: wupenga@mail.ustc.edu.cn (P. Wu).

0370-2693
doi:10.1016/j.physletb.2005.05.028

of the Higgs boson mass can be canceled by loop diagrams involving the supersymmetric partners of the SM particles exactly. The most attractive and simplest supersymmetric extension of the SM is the minimal supersymmetric standard model (MSSM) [2,3]. In this model, there are two Higgs doublets H_1 and H_2 to give masses to up- and down-type fermions. The Higgs sector consists of three neutral Higgs bosons, one CP-odd particle (A^0), two CP-even particles (h^0 and H^0), and a pair of charged Higgs bosons ($H^{\pm}$).

However, these Higgs bosons have not been directly explored experimentally until now. The published experimental lower mass bounds for the Higgs bosons presented by LEP experiments are: $M_{h^0} > 114.4$ GeV (at 95% CL) for the SM Higgs boson, and for the MSSM bosons $M_{h^0} > 91.0$ GeV and $M_{A^0} > 91.9$ GeV (at 95% CL, $0.5 < \tan\beta < 2.4$ excluded). The SM fits to precision electroweak data [4] indirectly set a limitation of the light Higgs boson, $M_{h^0} < 200$ GeV, while there should has a scalar Higgs boson lighter than about 130 GeV in MSSM [5]. This lightest Higgs boson with mediate mass is certainly in the exploring mass range of the present and future colliders, such as the Tevatron Run II, LHC and LC. At a LC the cross section for $e^+e^- \to t\bar{t}h$ is small, about 1 fb for $\sqrt{s} = 500$ GeV and $m_h = 100$ GeV [6,7]. But it has a distinctive experimental signature and can potentially be used to measure the top quark Yukawa coupling in the intermediate Higgs mass region at a LC with very high luminosity. Dawson and Reina calculated the NLO QCD corrections to $e^+e^- \to t\bar{t}h^0$ process at LC's in Ref. [8]. And in Refs. [9–11] the SM electroweak corrections to the process $e^+e^- \to t\bar{t}h^0$ are calculated. Chen et al., have studied the QCD and electroweak corrections to the process $\gamma\gamma \to t\bar{t}h^0$ in the SM at LC's [12]. All these works show that the evaluation of radiative corrections is a crucial task for all accurate measurements of $t\bar{t}h^0$ production process.

There are various channels which can be exploited to search for the Higgs boson h^0 with intermediate mass at TeV energy scale hadron colliders, such as gluon–gluon fusion Higgs boson production ($gg \to h^0$), the associated production with a weak intermediate boson ($qq' \to Wh^0, Zh^0$). Recently, the production channels $pp/p\bar{p} \to t\bar{t}h^0 + X$ attracted the physicist's attentions, because these channels offer a spectacular signature ($W^+W^-b\bar{b}b\bar{b}$) [13] and provides a possibility in probing the Yukawa coupling [14,15]. The total cross section for $pp/p\bar{p} \to t\bar{t}h^0 + X$ at tree level and NLO QCD corrections in the SM have been studied in Refs. [14–18].

The supersymmetric (SUSY) electroweak corrections to the $e^+e^- \to t\bar{t}h^0$ process can be over ten percent for favorable parameter values [19]. In Ref. [20], it was found that the SUSY QCD interactions by exchanging gluinos and squarks can impact on the Yukawa coupling vertex in the process $e^+e^- \to t\bar{t}h^0$ at LC. At $pp/p\bar{p}$ hadron colliders with a center-of-mass energy of TeV scale, the dominated contributions to $t\bar{t}h^0$ production are from subprocesses $q\bar{q}, gg \to t\bar{t}h^0$. To these high energy $t\bar{t}h^0$ production processes, the SUSY radiative corrections, especially the SUSY QCD corrections, may be remarkable.

In this Letter, we calculated the cross section for the associated production of the Higgs boson with top quark pair in the MSSM at hadron colliders including the NLO QCD corrections. In Section 2, we present the calculations of the leading order cross sections to $pp/p\bar{p} \to t\bar{t}h^0 + X$ in the MSSM. In Section 3, we present the calculations of the $\mathcal{O}(\alpha_s^3)$ QCD corrections to $pp/p\bar{p} \to t\bar{t}h^0 + X$ in the MSSM. The numerical results and discussions are presented in Section 4. Finally, a short summary is given.

2. The leading order cross sections

The Feynman diagrams at leading order (LO) for the subprocess

$$q(p_1)\bar{q}(p_2) \to t(k_1)\bar{t}(k_2)h^0(k_3), \tag{2.1}$$

in the MSSM are plotted in Fig. 1. They are s-channel, gluon exchange diagrams with Higgs boson radiation off top-quark and anti-top-quark, respectively. The process

$$g(p_1)g(p_2) \to t(k_1)\bar{t}(k_2)h^0(k_3), \tag{2.2}$$

at the tree level in the MSSM are described by the Feynman diagrams of Fig. 2. The LO Feynman diagrams for

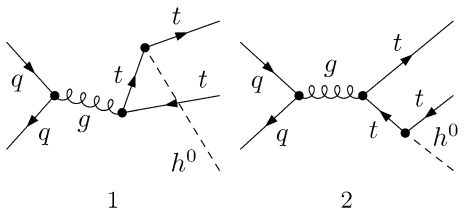

Fig. 1. The tree-level Feynman diagrams for the $q\bar{q} \to t\bar{t}h$ subprocess.

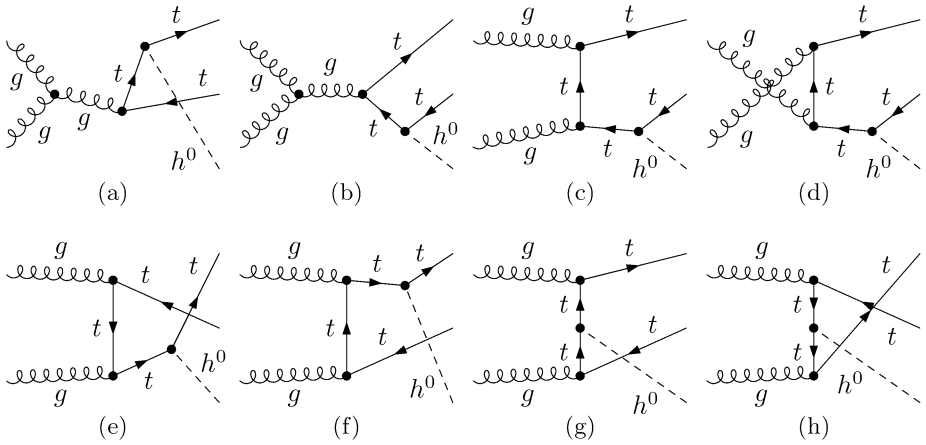

Fig. 2. The tree-level Feynman diagrams for the $gg \to t\bar{t}h$ subprocess.

both subprocesses in the MSSM are the same with their corresponding ones in the SM. In above two channels we use $p_{1,2}$ and $k_{1,2,3}$ to represent the four-momenta of the incoming partons and the outgoing particles, respectively. Because of the small mass of u- and d-quark, we neglect the diagrams which involve h^0–u–$\bar{u}$ and h^0–d–$\bar{d}$ Yukawa vertexes.

The explicit expression for the amplitudes of subprocess $q\bar{q} \to t\bar{t}h^0$ at tree level can be written as

$$M_{\mathrm{LO}}^{q\bar{q}} = A\bar{v}_k(p_2)\gamma_\mu u_i(p_1)\frac{ig_{\mu\nu}}{\hat{s}}\bar{u}_j(k_1)\frac{\not{k}_1 + \not{k}_3 + m_t}{(k_1+k_3)^2 - m_t^2}\gamma_\nu v_l(k_2)T_{ik}^a T_{jl}^b + (k_1 \leftrightarrow k_2), \tag{2.3}$$

where $\hat{s} = (p_1+p_2)^2$, T^a is the $SU(3)$ color matrix, $A = g_s^2 Y_{tth}^{(\mathrm{SUSY})}$. g_s is the strong coupling constant. $Y_{tth}^{(\mathrm{SUSY})}$ is the Yukawa coupling between Higgs boson and top quarks in the MSSM. As we know the h^0–t–$\bar{t}$ Yukawa coupling in the SM $Y_{tth}^{(\mathrm{SM})}$ is expressed by

$$Y_{tth}^{(\mathrm{SM})} = -ig_w\frac{m_t}{2m_W}. \tag{2.4}$$

But in the MSSM, $Y_{tth}^{(\mathrm{SUSY})}$ is given as

$$Y_{tth}^{(\mathrm{SUSY})} = -ig_w\frac{m_t}{2m_W}\frac{\cos\alpha}{\sin\beta}, \tag{2.5}$$

where α is the mixing angle which leads to the physical Higgs boson eigenstates h^0 and H^0. The angle β is defined as $\tan\beta = v_2/v_1$, where v_1 and v_2 are the vacuum expectation values.

According to the different topologies of Feynman diagrams, the explicit expression for the amplitudes of subprocess $gg \to t\bar{t}h^0$ in the MSSM at tree level can be divided into three parts:

$$M_{\rm tree}^{gg} = M_{\rm tree}^{gg1} + M_{\rm tree}^{gg2} + M_{\rm tree}^{gg3}, \tag{2.6}$$

where $M_{\rm tree}^{gg1}$, $M_{\rm tree}^{gg2}$ and $M_{\rm tree}^{gg3}$ correspond to the amplitudes of Fig. 2(a–b), Fig. 2(c–f) and Fig. 2(g–h), respectively. For the amplitude parts $M_{\rm tree}^{ggi}$ $(i = 1, 2, 3)$, we have the expressions as:

$$M_{\rm tree}^{gg1} = A f^{abc} T_{ij}^{c} \bar{u}_j(k_1) \frac{\not\epsilon_1^{\mu} \not\epsilon_2^{\nu}}{\hat{s}} \left[2p_1^{\nu} g^{\lambda\mu} + (p_2 - p_1)^{\lambda} g^{\mu\nu} - 2p_2^{\mu} g^{\nu\lambda}\right] \frac{-\not k_2 - \not k_3 + m_t}{2k_2 \cdot k_3 + m_{h^0}^2} v_i(k_2) + (k_1 \leftrightarrow k_2), \tag{2.7}$$

$$M_{\rm tree}^{gg2} = -i A T_{ik}^{a} T_{kj}^{b} \bar{u}_j(k_1) \frac{\not k_3 + \not k_1 + m_t}{2k_3 \cdot k_1 + m_{h^0}^2} \not\epsilon_2 \frac{-\not k_2 + \not p_1 + m_t}{-2k_2 \cdot p_1} \not\epsilon_1 v_i(k_2) + \begin{pmatrix} p_1 \leftrightarrow p_2, \epsilon_1 \leftrightarrow \epsilon_2 \\ p_1 \leftrightarrow p_2, \epsilon_1 \leftrightarrow \epsilon_2, k_1 \leftrightarrow k_2 \\ k_1 \leftrightarrow k_2 \end{pmatrix}, \tag{2.8}$$

$$M_{\rm tree}^{gg3} = -i A T_{ik}^{a} T_{kj}^{b} \bar{u}_j(k_1) \not\epsilon_2 \frac{\not k_1 - \not p_2 + m_t}{-k_1 \cdot p_2} \frac{-\not k_2 + \not p_1 + m_t}{-k_2 \cdot p_1} \not\epsilon_1 v_i(k_2) + (p_1 \leftrightarrow p_2, \epsilon_1 \leftrightarrow \epsilon_2), \tag{2.9}$$

where ϵ_1^{μ} and ϵ_2^{ν} are the polarization four-vectors of the incoming gluons. The $SU(3)$ structure constants are given by f_{abc}. Then the lowest order cross sections for the subprocesses $q\bar{q}, gg \to t\bar{t}h^0$ in the MSSM are obtained by using the following formula:

$$\hat{\sigma}_{\rm LO}^{q\bar{q},gg} = \frac{1}{2|\vec{k}_1|\sqrt{\hat{s}}} \int d\Phi_3 \overline{\sum} \left| M_{\rm tree}^{q\bar{q},gg} \right|^2, \tag{2.10}$$

where $d\Phi_3$ is the three-body phase space element. The summation is taken over the spins and colors of initial and final states, and the bar over the summation recalls averaging over the spins and colors of initial partons. The LO total cross section of $pp/p\bar{p} \to t\bar{t}h^0 + X$ can be expressed as

$$\sigma_{\rm LO}\left(pp/p\bar{p} \to t\bar{t}h^0 + X\right) = \sum_{ij} \int dx_1\, dx_2\, G_i^p(x_1, \mu) G_j^{p/\bar{p}}(x_2, \mu) \hat{\sigma}_{\rm LO}^{ij}(x_1, x_2, \mu), \tag{2.11}$$

where $\hat{\sigma}_{\rm LO}^{ij}$ $(ij = q\bar{q}, gg)$ is the LO parton-level total cross section for incoming i and j partons, $G_i^{p/\bar{p}}$'s are the LO parton distribution functions (PDF) with parton i in a proton/antiproton.

From the above deduction, we can see that the ratio between the tree level cross sections of subprocess $q\bar{q}(gg) \to t\bar{t}h^0$ in the SUSY model and the SM, is written as

$$\frac{\hat{\sigma}_{\rm LO}^{(\rm SUSY)}(q\bar{q}, gg \to t\bar{t}h^0)}{\hat{\sigma}_{\rm LO}^{(\rm SM)}(q\bar{q}, gg \to t\bar{t}h^0)} = \frac{\cos^2\alpha}{\sin^2\beta}. \tag{2.12}$$

3. NLO QCD corrections in the MSSM

In the calculation of the NLO QCD corrections in the MSSM, we adopt the dimensional regularization in $D = 4 - 2\epsilon$ dimensions to isolate the ultraviolet (UV), infrared (IR) and collinear singularities. Renormalization and factorization are performed in the modified minimal substraction ($\overline{\rm MS}$) scheme, and the wave functions of the external fields, and top quark's mass in propagators and in the Yukawa couplings are renormalized in the on-shell (OS) scheme. We divide the $\mathcal{O}(\alpha_s^3)$ QCD correction to the subprocess $q\bar{q}(gg) \to t\bar{t}h^0$ in the MSSM into two

parts. One is the so-called SM-like QCD correction part, another is SUSY-QCD correction part arising from virtual gluino/squark exchange contributions. Then the total NLO QCD corrections and relative corrections in the MSSM can be expressed as

$$\Delta\hat{\sigma}_{\rm NLO}^{(q\bar{q},gg)} = \Delta\hat{\sigma}_{\rm SM\text{-}like}^{(q\bar{q},gg)} + \Delta\hat{\sigma}_{\rm SQCD}^{(q\bar{q},gg)}, \qquad \hat{\delta}^{(q\bar{q},gg)} = \hat{\delta}_{\rm SM\text{-}like}^{(q\bar{q},gg)} + \hat{\delta}_{\rm SQCD}^{(q\bar{q},gg)}, \tag{3.1}$$

where we define the relative correction as $\hat{\delta} = \frac{\Delta\hat{\sigma}_{\rm NLO}}{\hat{\sigma}_{\rm LO}}$. The NLO SM-like QCD correction part (relative correction part) in the MSSM has following relation with the NLO SM QCD one

$$\Delta\hat{\sigma}_{\rm SM\text{-}like} = \left(\frac{\cos\alpha}{\sin\beta}\right)^2 \Delta\hat{\sigma}_{\rm SM}, \qquad \hat{\delta}_{\rm SM\text{-}like} = \hat{\delta}_{\rm SM}. \tag{3.2}$$

In our calculation we introduce the following counterterms:

$$\begin{aligned}
&m_t \to m_t + \delta m_t, \qquad g_s \to g_s + \delta g_s,\\
&t_L \to \left(1 + \frac{1}{2}\delta Z_L^t\right) t_L, \qquad t_R \to \left(1 + \frac{1}{2}\delta Z_R^t\right) t_R,\\
&u_L \to \left(1 + \frac{1}{2}\delta Z_L^u\right) u_L, \qquad u_R \to \left(1 + \frac{1}{2}\delta Z_R^u\right) u_R,\\
&d_L \to \left(1 + \frac{1}{2}\delta Z_L^d\right) d_L, \qquad d_R \to \left(1 + \frac{1}{2}\delta Z_R^d\right) d_R,\\
&G_\mu \to \left(1 + \frac{1}{2}\delta Z_g\right) G_\mu,
\end{aligned} \tag{3.3}$$

where g_s denotes the strong coupling constant, t, u, d and G_μ denote the fields of top-, up-, down-quark and gluon. The definitions and the explicit expressions of these renormalization constants can be found in Ref. [21]. For the renomalization of the QCD coupling constant g_s, we use the $\overline{\rm MS}$ scheme except that the divergences associated with the colored SUSY particle loops are subtracted at zero momentum [22]. Since we have $\delta g = \delta g^{(\rm SM\text{-}like)} + \delta g^{(\rm SQCD)}$, the terms should be obtained as

$$\frac{\delta g_s^{(\rm SM\text{-}like)}}{g_s} = -\frac{\alpha_s(\mu_r^2)}{4\pi}\left[\frac{\beta_0^{(\rm SM\text{-}like)}}{2}\frac{1}{\bar{\epsilon}} + \frac{1}{3}\ln\frac{m_t^2}{\mu_r^2}\right], \tag{3.4}$$

$$\frac{\delta g_s^{(\rm SQCD)}}{g_s} = -\frac{\alpha_s(\mu_r^2)}{4\pi}\left[\frac{\beta_0^{(\rm SQCD)}}{2}\frac{1}{\bar{\epsilon}} + \frac{N}{3}\ln\frac{m_{\tilde{g}}^2}{\mu_r^2} + \sum_{U=u,c,t}^{i=1,2}\frac{1}{12}\ln\frac{m_{\tilde{U}_i}^2}{\mu_r^2} + \sum_{D=d,s,b}^{j=1,2}\frac{1}{12}\ln\frac{m_{\tilde{D}_j}^2}{\mu_r^2}\right], \tag{3.5}$$

where

$$\beta_0^{(\rm SM\text{-}like)} = \frac{11}{3}N - \frac{2}{3}n_f - \frac{2}{3}, \qquad \beta_0^{(\rm SQCD)} = -\frac{2}{3}N - \frac{1}{3}(n_f + 1), \tag{3.6}$$

$N = 3$, $n_f = 5$ and $1/\bar{\epsilon} = 1/\epsilon_{\rm UV} - \gamma_E + \ln(4\pi)$. The summation is taken over the indexes of squark and generation. The $\overline{\rm MS}$ scheme violates supersymmetry explicitly, and the $q\tilde{q}\tilde{g}$ Yukawa coupling $\hat{g}_s$, which should be the same with the qqg gauge coupling g_s in the supersymmetry, takes a finite shift at one-loop order as shown in Eq. (3.7) [23],

$$\hat{g}_s = g_s\left[1 + \frac{\alpha_s}{8\pi}\left(\frac{4}{3}N - C_F\right)\right], \tag{3.7}$$

with $N = 3$ and $C_F = 4/3$. In our numerical calculation we take this shift between $\hat{g}_s$ and g_s into account.

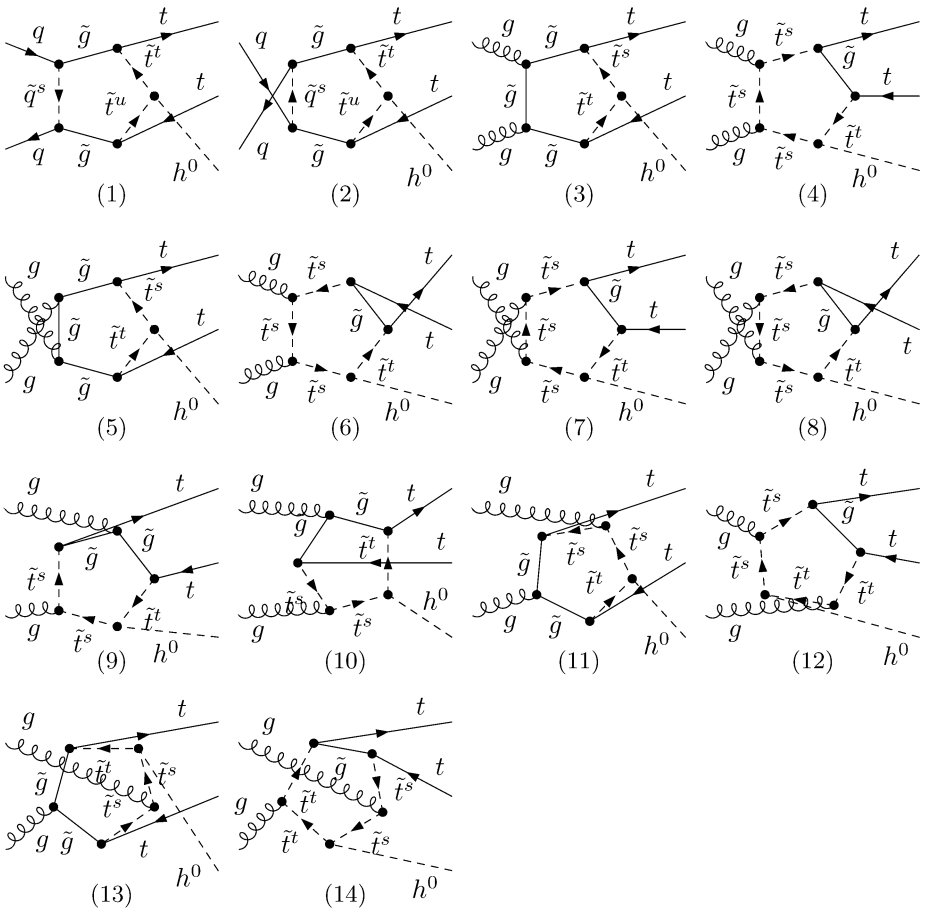

Fig. 3. The pentagon diagrams for the $q\bar{q} \to t\bar{t}h^0$ and $gg \to t\bar{t}h^0$ subprocess.

Actually, the calculation of the NLO SM-like QCD corrections in the MSSM for the subprocesses $q\bar{q}, gg \to t\bar{t}h^0$ is the same as that of the NLO SM QCD corrections in Refs. [14,15], except their numerical results satisfied the relations shown in Eq. (3.2).

The NLO SUSY-QCD contribution part to the $q\bar{q}(gg) \to t\bar{t}h^0$ subprocess comes from the one-loop diagrams involving virtual gluino/squark exchange. For demonstration, we show the pentagon diagrams which contribute to the NLO SUSY-QCD correction part for the subprocesses $q\bar{q} \to t\bar{t}h^0$ and $gg \to t\bar{t}h^0$ in Fig. 3, where the upper indexes $s, t, u = 1, 2$. Because there is no massless particle in the loop, all these diagrams with gluino/squark loop are IR finite. The pentagon and box diagrams in SUSY-QCD part are UV finite, but the self-energy and vertex diagrams in this part contain UV divergences. That is renormalized by the proper related counterterms defined in Eq. (3.3).

The $\mathcal{O}(\alpha_s^3)$ supersymmetric QCD correction part of the cross section in the MSSM to the subprocesses $q\bar{q}, gg \to t\bar{t}h^0$ can be expressed as

$$\Delta\hat{\sigma}_{\mathrm{SQCD}}^{(q\bar{q},gg)} = \frac{1}{2|\vec{k}_1|\sqrt{\hat{s}}} \int d\Phi_3 \overline{\sum} 2\,\mathrm{Re}\big(\mathcal{M}_{\mathrm{tree}}^{(q\bar{q},gg)} \mathcal{M}_{\mathrm{SQCD}}^{(q\bar{q},gg)\dagger}\big), \tag{3.8}$$

where $\mathcal{M}_{\mathrm{tree}}^{(q\bar{q},gg)}$ are the Born amplitudes for $q\bar{q}, gg \to t\bar{t}h^0$ subprocesses, and $\mathcal{M}_{\mathrm{SQCD}}^{(q\bar{q},gg)}$ are the renormalized amplitudes of all the one-loop Feynman diagrams involving virtual gluino/squark.

In the calculations of loop diagrams we adopt the definitions of one-loop integral functions of Ref. [24]. The Feynman diagrams and the relevant amplitudes are generated by FeynArts3 [25], and the Feynman amplitudes are subsequently reduced by FormCalc32 [26]. The phase space integration is implemented by using Monte Carlo technique. The numerical calculations of integral functions are implemented by using developed LoopTools [27].

We write the NLO QCD corrected parton-level total cross section $\hat{\sigma}^{ij}_{\rm NLO}(x_1, x_2, \mu)$ as

$$\hat{\sigma}^{(q\bar{q},gg)}_{\rm NLO} \equiv \hat{\sigma}^{(q\bar{q},gg)}_{\rm LO} + \Delta\hat{\sigma}^{(q\bar{q},gg)}_{\rm NLO}.$$

The NLO QCD corrected total cross section of $pp/p\bar{p} \to t\bar{t}h^0 + X$ in the MSSM can be expressed as:

$$\sigma_{\rm NLO}\big(pp/p\bar{p} \to t\bar{t}h^0\big) = \sum_{ij} \int dx_1\, dx_2\, G^p_i(x_1,\mu) G^{p/\bar{p}}_j(x_2,\mu) \hat{\sigma}^{(ij)}_{\rm NLO}(x_1, x_2, \mu), \tag{3.9}$$

where $\hat{\sigma}^{(ij)}_{\rm NLO}$ $(ij = q\bar{q}, gg)$ is the NLO QCD corrected parton-level total cross section for incoming i and j partons, and $G^{p/\bar{p}}_i$ are the NLO parton distribution functions (PDF) for parton i in a proton/antiproton. The equation include two channels: $q\bar{q}, gg \to t\bar{t}h^0$. In our calculations, we choose the factorization scale equals the renormalization scale, i.e., $\mu_f = \mu_r = Q$. The partonic center-of-mass energy squared, $\hat{s}$, is given in terms of the total hadronic center-of-mass energy squared $\hat{s} = x_1 x_2 s$.

4. Numerical results and discussion

In our numerical calculation, we adopt the MRST NLO parton distribution function [28] and the 2-loop evolution of $\alpha_s(\mu^2)$ to evaluate the hadronic NLO QCD corrected cross sections, while for the hadronic LO cross sections we use the MRST LO parton distribution function and the one-loop evolution of $\alpha_s(\mu^2)$. We take the SM parameters as $\alpha_{\rm ew}(m_Z^2)^{-1} = 127.918$, $m_W = 80.423$ GeV, $m_Z = 91.188$ GeV, $m_t = 174.3$ GeV, $m_u = m_d = 66$ MeV [29]. There we use the effective values of the light quark masses (m_u and m_d) which can reproduce the hadron contribution to the shift in the fine structure constant $\alpha_{\rm ew}(m_Z^2)$ [30]. The other relevant parameters, such as mixing angle of the Higgs fields α and masses of the lightest Higgs boson, gluino, stop-quarks, are obtained by adopting the FormCalc package, except otherwise stated. The input parameters for the FormCalc program are M_S, M_2, A_t, m_{A^0}, μ and $\tan\beta$. The related parameters for the MSSM Higgs sector are obtained from the CP-odd mass m_{A^0} and $\tan\beta$ with the constraint $\tan\beta \geqslant 2.5$. In the program the grand unification theory (GUT) relation $M_1 = (5/3)\tan^2\theta_W M_2$ is adapted for simplification and the gluino mass $m_{\tilde{g}}$ is evaluated by $m_{\tilde{g}} = \alpha_s(Q)/\alpha_{\rm ew}(m_Z)\sin^2\theta_W M_2$. For the sfermion sector, the relevant input parameters are M_S, A_f and μ, and there we take the assumptions of $M_Q = M_U = M_D = M_E = M_L = M_S$ and the soft trilinear couplings for sfermions $\tilde{q}$ and $\tilde{l}$ being equal, i.e., $A_q = A_l = A_f$.

We present the dependence of the cross section on the renormalization/factorization scale Q/Q_0 in Fig. 4(a–b) for the Tevatron and the LHC separately, where we denote $Q_0 = m_t + m_{h^0}/2$ and the input parameters are taken as $A_t = 800$ GeV, $M_S = 400$ GeV, $M_2 = 110$ GeV, $m_{A^0} = 270$ GeV, $\mu = -200$ GeV and $\tan\beta = 6$. With these input parameters, we get all the other supersymmetric parameters, among them $\cos\alpha = 0.954$, $m_{h^0} = 120$ GeV, $m_{\tilde{t}_1} = 207.75$ GeV and $m_{\tilde{t}_2} = 577.63$ GeV, but the value of $m_{\tilde{g}}$ is a function of the energy scale Q ($m_{\tilde{g}}(Q_0) = 317.9$ GeV). In order to show the cross section dependence on the renormalization/factorization scale, we fix $m_{\tilde{g}} = 300$ GeV in Fig. 4(a–b). There we plot the curves for cross sections $\sigma_{\rm LO}$, $\sigma_{\rm NLO}$ and $\sigma^{\rm SM\text{-}like}_{\rm NLO}$ of the processes $p\bar{p}/pp \to t\bar{t}h^0 + X$. The notations $\sigma_{\rm NLO}$ and $\sigma^{\rm SM\text{-}like}_{\rm NLO}$ represent the cross sections involving complete QCD and SM-like QCD corrections. Fig. 4(a) shows that the NLO QCD contributions to the process $p\bar{p} \to t\bar{t}h^0 + X$ in the MSSM at the Tevatron, in which the dominant subprocess is $q\bar{q} \to t\bar{t}h^0$, has a negative NLO QCD corrections near the position of $Q = Q_0$. While Fig. 4(b) shows that the NLO QCD contributions to the process $pp \to t\bar{t}h^0 + X$ in the MSSM at the LHC, in which the dominant subprocess is $gg \to t\bar{t}h^0$, will give positive corrections near the

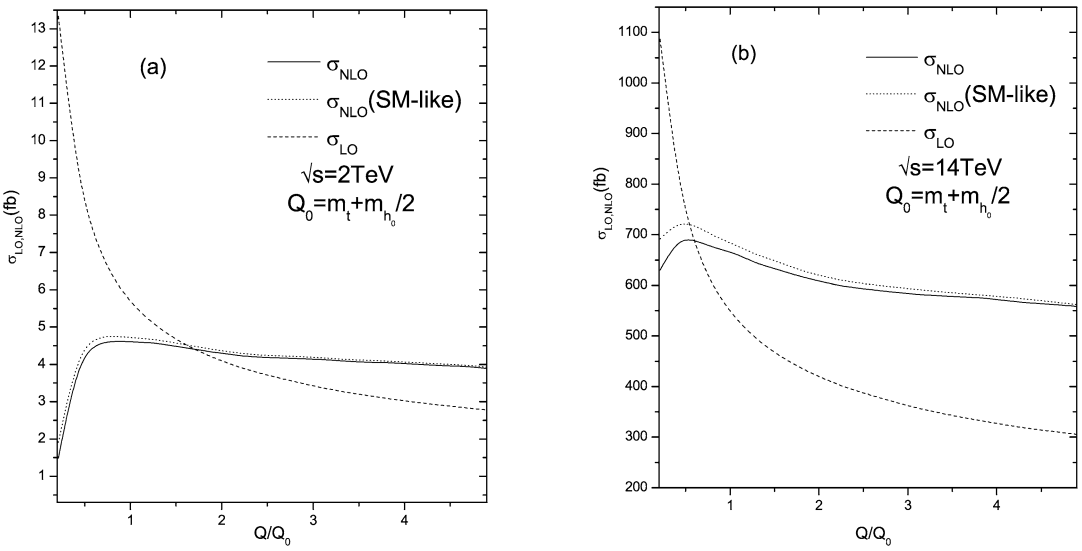

Fig. 4. The cross sections $\sigma_{\rm LO}$ at the leading order and $\sigma_{\rm NLO}$ involving the NLO QCD corrections in the MSSM as the functions of the renormalization/factorization scale Q with $m_{\tilde{g}} = 300$ GeV and the other parameters are from FormCalc by using the input SUSY parameters: $M_S = 400$ GeV, $M_2 = 110$ GeV, $A_t = 800$ GeV, $m_{A^0} = 270$ GeV, $\mu = -200$ GeV and $\tan\beta = 6$. (a) is for the process $p\bar{p} \to t\bar{t}h^0 + X$ at the Tevatron and (b) for the process $pp \to t\bar{t}h^0 + X$ at the LHC.

position of $Q = Q_0$. Here we should note that if Q goes down to a very low value, i.e., $Q \ll Q_0$, large logarithmic corrections spoil the convergence of perturbation theory in the proton–antiproton colliding energy of the Tevatron. That can be seen from our numerical results for the Tevatron. It shows that the total NLO QCD corrected cross section $\sigma_{\rm NLO}$ in the MSSM tends to have a negative value when $Q \to 0$ [15]. From Fig. 4(a–b), we can conclude that the dependence of the NLO QCD corrected cross section $\sigma_{\rm NLO}$ on the scale Q is significantly reduced comparing with $\sigma_{\rm LO}$, and is slightly weakened comparing with $\sigma_{\rm NLO}^{\rm SM\text{-}like}$.

In the following calculation, we fixed the value of the renormalization/factorization scale being Q_0. In Fig. 5(a, b) we show the LO and total NLO QCD cross sections $\sigma_{\rm LO}$ and $\sigma_{\rm NLO}$ in the MSSM as the functions of $\tan\beta(m_{h^0})$ at the Tevatron and the LHC respectively, taking $A_t = 800$ GeV, $M_S = 400$ GeV, $M_2 = 110$ GeV, $m_{A^0} = 270$ GeV and $\mu = -200$ GeV. The corresponding relative corrections δ of both cross sections versus $\tan\beta(m_{h^0})$, where the relative correction is defined as $\delta = \frac{\sigma_{\rm NLO} - \sigma_{\rm LO}}{\sigma_{\rm LO}}$, are plotted in Fig. 5(c). From these figures, we can see that the cross sections $\sigma_{\rm NLO}$ and $\sigma_{\rm LO}$ decrease rapidly as $\tan\beta$ varies in the range from 2 to 10, and then goes down very slowly when $\tan\beta$ changes from 10 to 40. We can read from Fig. 5(a–b) that when $\tan\beta$ increases from 2 to 40, the total NLO QCD corrected cross section $\sigma_{\rm NLO}$ in the MSSM decreases roughly from 9.1 fb and 1078 fb to 5.2 fb and 641 fb for the Tevatron and the LHC, respectively. The two curves of relative corrections δ for the Tevatron and the LHC in Fig. 5(c) look like rather stable when $\tan\beta$ runs from 2 to 50. We can read from this figure that the NLO QCD relative correction values in the MSSM at the Tevatron and the LHC are generally about -17% and 26% in these varying range of $\tan\beta$, respectively.

In Fig. 6, we show the relative NLO QCD correction δ in the MSSM as a function of M_S, taking $A_t = 800$ GeV, $M_2 = 110$ GeV, $m_{A^0} = 270$ GeV, $\mu = -200$ GeV and $\tan\beta = 6$. The figure demonstrates that the relative NLO QCD corrections in the MSSM at the Tevatron and the LHC, are stable when M_S changes from 400 GeV to 2 TeV. Their values are about 25% at the LHC and -18% at the Tevatron. We find from our calculation that when M_S is taken as a large value, the correction from the NLO SUSY QCD correction part decreases to a constant due to the decouple of heavy stop quarks.

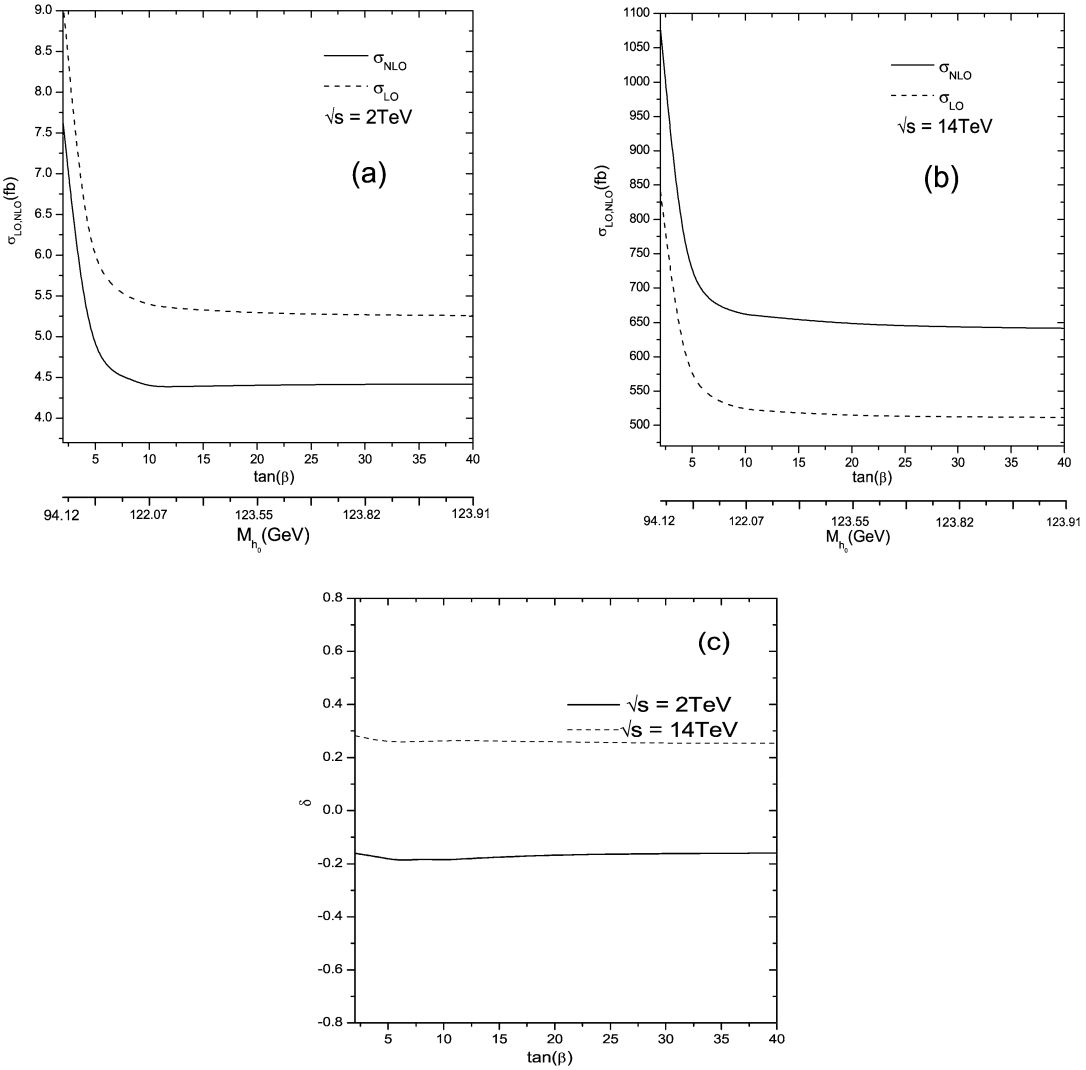

Fig. 5. The cross sections $\sigma_{\rm LO}$ at the leading order and $\sigma_{\rm NLO}$ involving the NLO QCD corrections in the MSSM as the functions of $\tan\beta$ with the input parameters $A_t = 800$ GeV, $M_2 = 110$ GeV, $m_{A^0} = 270$ GeV, $M_S = 400$ GeV, $\mu = -200$ GeV. (a) is for the process $p\bar{p} \to t\bar{t}h^0 + X$ at the Tevatron and (b) for the process $pp \to t\bar{t}h^0 + X$ at the LHC. (c) shows the relative NLO QCD correction as the function of $\tan\beta$ in both the Tevatron and LHC.

Fig. 7 shows the total QCD relative correction δ in the MSSM as a function of $m_{\tilde{g}}$ with the input parameters same as in Fig. 4. We can see from this figure that the δ have a concave structure in the vicinity of $m_{\tilde{g}} \sim 140$–150 GeV, where the masses satisfy the relation $m_{\tilde{g}} + m_t \approx m_{\tilde{t}_1} + m_{h^0}$ and the re-scattering enhancement $\tilde{t}_1^* \to \tilde{g} + t \to \tilde{t}_1 + h^0$ takes place. When $m_{\tilde{g}}$ goes from 400 GeV to 2000 GeV, the relative corrections are very stable, they are about 24% for the LHC and -18% for the Tevatron. Similar with the case in Fig. 6, due to the decouple effect the correction of the SUSY QCD correction part decreases to a constant when $\tilde{g}$ is getting heavy.

Fig. 8 presents the total NLO QCD relative correction δ in the MSSM as a function of the SUSY parameter A_t, assuming $M_S = 400$ GeV, $M_2 = 110$ GeV, $m_{A^0} = 270$ GeV, $\mu = -200$ GeV and $\tan\beta = 6$. We can see from the figure that the total NLO QCD relative corrections in the MSSM are very sensitive to A_t in the region near

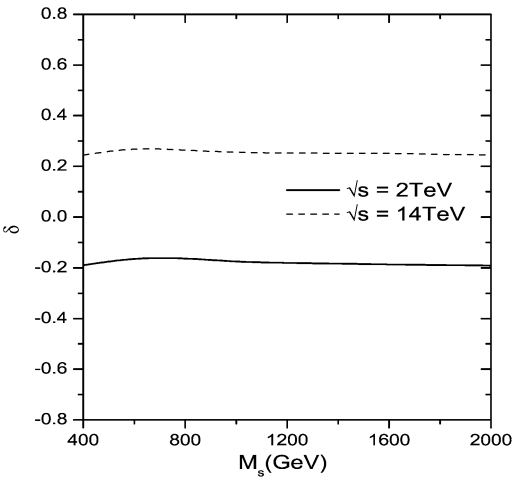

Fig. 6. The total NLO QCD relative corrections (δ) of the processes $p\bar{p}/pp \to t\bar{t}h^0 + X$ at the Tevatron and the LHC, as the functions of M_S.

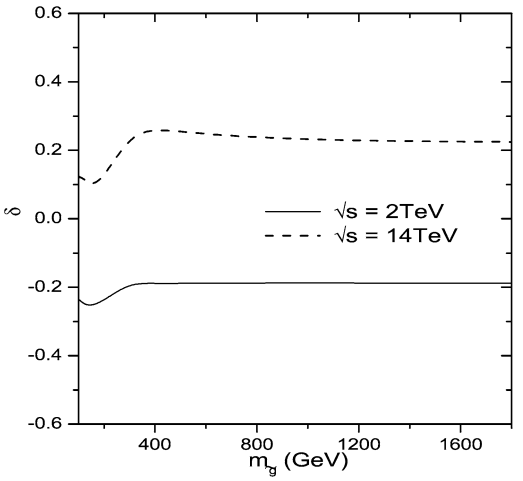

Fig. 7. The total NLO QCD relative corrections (δ) of the processes $p\bar{p}/pp \to t\bar{t}h^0 + X$ at the Tevatron and the LHC, as the functions of $m_{\tilde{g}}$.

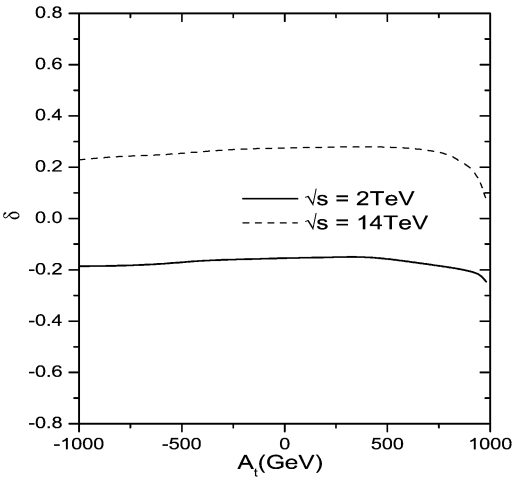

Fig. 8. The total NLO QCD relative corrections (δ) of the processes $p\bar{p}/pp \to t\bar{t}h^0 + X$ at the Tevatron and the LHC, as the functions of A_t.

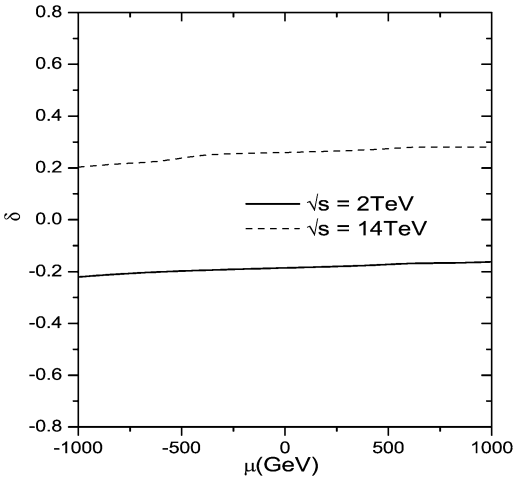

Fig. 9. The total NLO QCD relative corrections (δ) of the processes $p\bar{p}/pp \to t\bar{t}h^0 + X$ at the Tevatron and the LHC, as the functions of μ.

the position of $A_t = 1000$ GeV (where $m_{\tilde{t}_1} = 108.6$ GeV). Actually, the reason for that is because of the large contribution from the light stop quark $\tilde{t}_1$ loops. When the chosen parameters A_t and μ make a large mass splitting between the two scalar top-quarks, then the $\tilde{t}_1$ becomes light. We can read from the figure the total NLO QCD relative correction δ in the MSSM can reach -24% at the Tevatron and 7% at the LHC when A_t is near 1000 GeV.

In Fig. 9, we show the total NLO QCD relative correction δ in the MSSM as a function of the SUSY parameter μ, assuming $A_t = 800$ GeV, $M_S = 400$ GeV, $M_2 = 110$ GeV, $m_{A^0} = 270$ GeV and $\tan\beta = 6$. We can see that the total NLO QCD relative corrections in the MSSM increase slowly when μ goes up from -1000 GeV to 1000 GeV, this is because the absolute values of the negative corrections from the SUSY QCD part are becoming smaller as μ increases. The value of δ at the Tevatron can be beyond -22% when μ is about -1000 GeV.

In this Letter we calculated the NLO QCD corrections to the processes $p\bar{p}/pp \to t\bar{t}h^0 + X$ in the MSSM at the Tevatron and the LHC. We analyzed the dependence of the corrected cross sections or relative corrections on the renormalization/factorization scale Q, SUSY parameters $\tan\beta$, M_S, $m_{\tilde{g}}$, A_t and μ, respectively. It shows that the dependence of the total NLO QCD corrected cross section in the MSSM on the scale Q is significantly reduced comparing with the $\sigma_{\rm LO}$. With our chosen parameters, the numerical results demonstrate that the relative correction is obviously related to $m_{\tilde{g}}$, A_t and μ in some parameter regions, but not very sensitive to $\tan\beta$, M_S at both the Tevatron and the LHC for our specified parameters. We conclude that the total NLO QCD corrections are generally moderate, which have the values in the range of few percent to about 20% in most of the SUSY parameter space. We find that the relative correction from the NLO SUSY QCD correction part becomes to be constant when either M_S or $m_{\tilde{g}}$ has large value. We find also the relative correction of the SUSY QCD part will be largely enhanced when the mass splitting between stop-quarks is large, the total NLO QCD relative correction in the MSSM δ can reach -24% at the Tevatron and 7% at the LHC.

Acknowledgements

This work was supported in part by the National Natural Science Foundation of China and special fund sponsored by China Academy of Science.

References

[1] S. Weinberg, Phys. Rev. Lett. 19 (1967) 1264;
S. Glashow, Nucl. Phys. B 22 (1961) 579;
A. Salam, in: N. Svartholm (Ed.), Elementary Particle Theory, Almqvist and Wiksell, Stockholm, 1968, p. 367.
[2] H.P. Nilles, Phys. Rep. 110 (1984) 1;
H.E. Haber, G.L. Kane, Phys. Rep. 117 (1985) 75.
[3] J.F. Gunion, H.E. Haber, Nucl. Phys. B 272 (1986) 1.
[4] LEPEWWG/2001-01, May 2001.
[5] S. Heinemeyer, W. Hollik, G. Weiglein, Eur. Phys. J. C 9 (1999) 343, hep-ph/9812472.
[6] S. Dittmaier, M. Krämer, Y. Liao, M. Spira, P.M. Zerwas, Phys. Lett. B 441 (1998) 383.
[7] A. Juste, G. Merino, hep-ph/9910301.
[8] S. Dawson, L. Reina, Phys. Rev. D 59 (1999) 054012.
[9] Y. You, W.-G. Ma, H. Chen, R.-Y. Zhang, Y.-B. Sun, H.-S. Hou, Phys. Lett. B 571 (2003) 85, hep-ph/0306036.
[10] G. Belanger, F. Boudjema, J. Fujimoto, T. Ishikawa, T. Kaneko, K. Kato, Y. Shimizu, Y. Yasui, Phys. Lett. B 571 (2003) 163, hep-ph/0307029.
[11] A. Denner, S. Dittmaier, M. Roth, M.M. Weber, Phys. Lett. B 575 (2003) 290, hep-ph/0307193.
[12] H. Chen, W.-G. Ma, R.-Y. Zhang, P.-J. Zhou, H.-S. Hou, Y.-B. Sun, Nucl. Phys. B 683 (2004) 196.
[13] J. Goldstein, C.S. Hill, J. Incandela, S. Parke, D. Rainwater, D. Stuart, Phys. Rev. Lett. 86 (2001) 1694, hep-ph/0006311.
[14] L. Reina, S. Dawson, D. Wackeroth, Phys. Rev. D 65 (2002) 053017, hep-ph/0109066.
[15] W. Beenakker, S. Dittmaier, M. Kramer, B. Plumper, M. Spira, P.M. Zerwas, Phys. Rev. Lett. 87 (2001) 201805, hep-ph/0107081;
W. Beenakker, S. Dittmaier, M. Kramer, B. Plumper, M. Spira, P.M. Zerwas, Nucl. Phys. B 653 (2003) 151, hep-ph/0211352.
[16] Z. Kunszt, Nucl. Phys. B 247 (1984) 339;
W.J. Marciano, F.E. Paige, Phys. Rev. Lett. 66 (1991) 2433;
Z. Kunszt, S. Moretti, W.J. Stirling, Z. Phys. C 74 (1997) 479, hep-ph/9611397.
[17] D. Rainwater, M. Spira, D. Zeppenfeld, MAD-PH-02-1260, hep-ph/0203187.
[18] J. Goldstein, C.S. Hill, J. Incandela, S. Parke, D. Rainwater, D. Stuart, Phys. Rev. Lett. 86 (2001) 1694.
[19] X.-H. Wu, C.S. Li, J.J. Liu, hep-ph/0308012.
[20] S.-h. Zhu, hep-ph/0212273;
P. Haefliger, M. Spira, hep-ph/0501164.
[21] A. Denner, Fortschr. Phys. 41 (1993) 307.
[22] J. Collins, F. Wilczek, A. Zee, Phys. Rev. D 18 (1978) 242;
W.J. Marciano, Phys. Rev. D 29 (1984) 580;

W.J. Marciano, Phys. Rev. D 31 (1984) 213, Erratum;
P. Nason, S. Dawson, R.K. Ellis, Nucl. Phys. B 327 (1989) 49;
P. Nason, S. Dawson, R.K. Ellis, Nucl. Phys. B 335 (1989) 260, Erratum.
[23] W. Beenakker, R. Höpker, P.M. Zerwas, Phys. Lett. B 378 (1996) 159;
W. Beenakker, R. Höpker, T. Plehn, P.M. Zerwas, Z. Phys. C 75 (1997) 349.
[24] G. Passarino, M. Veltman, Nucl. Phys. B 160 (1979) 151.
[25] J. Kublbeck, M. Bohm, A. Denner, Comput. Phys. Commun. 60 (1990) 165;
T. Hahn, Comput. Phys. Commun. 140 (2001) 418.
[26] T. Hahn, M. Perez-Victoria, Comput. Phys. Commun. 118 (1999) 153.
[27] T. Hahn, Nucl. Phys. B (Proc. Suppl.) 89 (2000) 231;
A. Denner, S. Dittmaier, Nucl. Phys. B 658 (2003) 175.
[28] A.D. Martin, R.G. Roberts, W.J. Stirling, R.S. Thorne, Phys. Lett. B 531 (2002) 216, hep-ph/0201127;
A.D. Martin, R.G. Roberts, W.J. Stirling, R.S. Thorne, Eur. Phys. J. C 23 (2002) 73, hep-ph/0110215;
A.D. Martin, R.G. Roberts, W.J. Stirling, R.S. Thorne, Eur. Phys. J. C 28 (2003) 455, hep-ph/0211080.
[29] S. Eidelman, et al., Phys. Lett. B 592 (2004) 1.
[30] F. Legerlehner, DESY 01-029, hep-ph/0105283.